Published in final edited form as:
J Neurosci Methods. 2012 September 30; 210(2): 119–124. doi:10.1016/j.jneumeth.2012.07.019.

Optogenetic field potential recording in cortical slices

Wenhui Xiong and **Xiaoming Jin***
Department of Anatomy and Cell Biology, Stark Neuroscience Research Institute, Indiana Spinal Cord and Brain Injury Research Group, Indiana University School of Medicine, 980 W. Walnut Street, Indianapolis, IN 46202, USA.

Abstract

We introduce a method that uses optogenetic stimulation to evoke field potentials in brain slices prepared from transgenic mice expressing Channelrhodopsin2-YFP. Cortical slices in a recording chamber were stimulated with a 473 nm blue laser via either a laser scanning photostimulation setup or by direct guidance of a fiber optic. Field potentials evoked by either of the two optogenetic stimulation methods had stable amplitude, consistent waveform, and similar components as events evoked with a conventional stimulating electrode. The amplitude of evoked excitatory postsynaptic potentials increased with increasing laser intensity or pulse duration. We further demonstrated that optogenetic stimulation can be used for the induction and monitoring of long-term depression. We conclude that this technique allows for efficient and reliable activation of field potentials in brain slice preparation, and will be useful for studying short and long term synaptic plasticity.

Keywords

Field potential recording; optogenetics; Channelrhodopsin 2; cerebral cortex; brain slice; long-term depression

1. Introduction

Field potential recording (FPR) in brain slice preparation has been widely used as an efficient and reliable electrophysiological technique for studying synaptic transmission, network activities, and short-term and long-term synaptic plasticity under various physiological, pathological, and pharmacological conditions (Renshaw et al., 1940, Barrionuevo and Brown, 1983, Kimura et al., 1989, Prince and Tseng, 1993). These experiments typically involve activating neurons and axons in a brain slice with a stimulating electrode, and recoding evoked responses with one or multiple low impedance recording electrodes, allowing assessment of synaptic activities in a population of neurons in a brain region. However, there exist several limitations in this technique that often affect its application and the interpretation of results. For example, electrical stimulation evokes activities of both the nearby neurons and any en passant axons so that a small percentage of sparsely distributed neurons are activated (Histed et al., 2009), which makes it difficult to

*Corresponding author. Current address: Stark Neurosciences Research Institute, Indiana University School of Medicine, 980 W. Walnut Street, R3, Room C426B, Indianapolis, IN 46202. Tel: (317) 278-5766. xijin@iupui.edu.

determine the origin of the axons and the location of the neurons that contribute to the evoked synaptic responses. Technically, a deterioration of the electrical properties of a stimulating electrode (e.g. bubble or debris at the tip of a metal electrode) can significantly affect the amplitude and waveform of the evoked responses, which can make it difficult to determine whether the changes in the responses are due to changes in the efficacy of synaptic transmission or merely alterations in the properties of the stimulating electrode.

The recent optogenetic technology provides a revolutionary approach for precisely stimulating genetically defined neurons and axons. Neurons and their axons that express channelrhodposin-2 (ChR2) can be effectively activated to fire action potentials by exposure to blue light with high spatial and temporal precision(Boyden et al., 2005, Arenkiel et al., 2007, Wang et al., 2007). The unique advantages of optogenetic stimulation may help overcome some of the limitations of the traditional FPR discussed above and improve its application. A specialized dual-modality hybrid 'optrode' has recently been invented for simultaneous optogenetic stimulation and extracellular recording of neural activity for in vitro and in vivo applications (Wang et al., Zhang et al., 2009). However, a method that uses optogenetic stimulation to evoke responses in a regular FPR setup has not been demonstrated. In the present work, we describe a technique that used either a laser scanning photostimulation (LSPS) setup or simply a fiber optic for optogenetic field potential recording (oFPR) in cortical slices of ChR2-YFP expressing transgenic mice, and discuss its advantages, limitations, and potential applications.

2. Materials and methods

2.1 Brain slice preparation

Transgenic mice expressing ChR2-YFP under the control of Thy1 promoter (line 9, stock number 7615, Jackson lab) were used in all experiments (Arenkiel et al., 2007). Brain slices were cut from adult (postnatal days 40–60) mice using a procedure described previously (Jin et al., 2006, Jin et al., 2011). Briefly, mice were anesthetized with pentobarbital (55 mg/kg, i.p.) and decapitated. The brain was rapidly removed and submerged in ice-cold (4°C) oxygenated slicing solution containing (in mM): 230 sucrose, 2.5 KCl, 1.25 NaH_2PO_4, 10 $MgSO_4{\cdot}7HO_2$, 10 glucose, 0.5 $CaCl_2{\cdot}2H_2O$, and 26 $NaHCO_3$. Coronal slices (350 μm) containing the sensorimotor cortex were cut with a vibratome (Leica VT1200, Leica) in standard artificial cerebrospinal fluid (ACSF). The ACSF contained the following (in mM): 126 NaCl, 2.5 KCl, 1.25 NaH_2PO_4, 2 $CaCl_2{\cdot}2H_2O$, 2 $MgSO_4{\cdot}7H_2O$, 26 $NaHCO_3$, and 10 glucose, pH 7.4 when saturated with 95% O_2–5% CO_2. The slices were incubated at 35°C for 30 minutes, and were then maintained in a dark environment in oxygenated ACSF at room temperature.

2.2 Setup for optogenetic stimulation

We used two methods to position the beam of a blue laser (473 nm, 120 mW, OptoEngine LLC, Salt Lake, Utah) for optogenetic stimulation. In most experiments, an LSPS setup that is coupled with an upright microscope (Axio Examiner, Zeiss, Germany) was used to position the laser beam to a target location under a microscopic field (Fig. 1A)(Jin et al., 2006, Jin et al., 2011). Specifically, the laser was guided through a multi-modular fiber optic to mirror galvanometers (model 6210); Cambridge Technology, Cambridge, MA). The laser passed through a telescope consisting of a scan lens and a tube lens, was reflected by a dichroic mirror in the fluorescent turret, and projected onto the back aperture of a 5× objective. The microscopic field was imaged with an analog camera (4810 Series, Cohu Electronics Inc, Poway, CA) and displayed on the imaging window of scanning software that controlled the movement of the galvanometers for positioning of the laser beam on a grid (Fig. 1 A and D).

Alternatively, we guided the blue laser with a customized multi-modular fiber optic (200 μm core diameter, 1 meter long, numeric aperture 0.37, Thorlabs, Newtown, NJ). The fiber patch cable consisted of an FC/PC connector and an end with flat cleave, and was unjacketed for precise positioning. A micromanipulator was used to position the fiber optic to target a spot on a slice (e.g. white matter) (Fig. 1B and E). This method was very cost-effective and easy to prepare, and was similar to the conventional electrode positioning method except that the fiber optic did not physically touch the surface of the slice.

A pulse generator was used to control the patterns and duration of the laser pulses. The laser intensity was attenuated with a circular variable neutral density filter on the light path (100 mm diameter, 0–2.0 optical density, Newport, Irvine, CA. Fig. 1A–B). The maximum power of a 1 ms pulse under the objective was measured at ~0.04–0.07 mW when the filter was set to minimum attenuation. The laser spot under the objective had a diameter of ~ 80 μm.

2.3 Optogenetic stimulation and field potential recording

Extracellular field potentials were recorded in either a submerged chamber or an interface chamber using glass micropipettes pulled from borosilicate glass. After the tips were broken, the pipettes had a resistance of 0.5–1 MΩ when filled with ACSF. The recording pipettes were positioned on cortical layer II/III or layer V of the slices. Optogenetic stimuli consisted of a brief pulse of blue laser with 0.01–0.04 mW power under the objective and 0.01–5 ms duration, and were delivered onto the white matter or layer V to evoke responses. oFPRs were made with the use of a multiClamp amplifier (700B, Molecular Device, Sunnyvale, CA). Signals were filtered at 1 kHz, digitized at 10 kHz, and saved on a computer.

For comparison between electrical and optogenetic stimulation, electrical stimulation was made with a concentric bipolar electrode, which was placed on the border between layer VI and white matter of the cortical slices. Stimuli were comprised of a biphasic pulse (0.2 ms, 20–800 μA) generated by an isolated stimulator (Model 2200), A-M system, WA).

2.4 Induction of long-term and depression (LTD)

For LTD recording, we applied optogenetic stimulation onto the layer V and placed a recording electrode on layer II/III. LTD induction was made after stable baseline oFPRs were obtained at 0.033 Hz for at least 15 minutes. Low frequency stimulation (LFS, 1 ms, 0.04 mW, 900 pulses at 1 Hz) or another conditioning stimulation at 2 or 4 Hz was applied to the white matter or layer V of the slices, using the same stimulation intensity as the testing stimuli. After cessation of conditioning stimulation, changes in field potentials were monitored using 0.033 Hz stimulation for 60 min.

2.5 Data analysis

The peak amplitudes of field excitatory postsynaptic potentials (fEPSPs) or inhibitory postsynaptic potentials (fIPSPs) were measured as the differences from baselines to the peaks of the field waveforms. For LTD experiments, the baseline fEPSP amplitudes were obtained from the averaged field potentials recorded for 5 min immediately before LFS. The amplitudes after LFS were measured and normalized to those of the baseline responses. The magnitudes of LTD were evaluated as the relative changes in fEPSPs recorded 60 min after LFS.

3. Results

3.1 Field potentials evoked by optogenetic stimulation

In all the experiments, we used coronal slices of the sensorimotor cortex prepared from the adult ChR2-YFP expressing mice, in which the somata and apical dendrites of cortical layer

V pyramidal neurons strongly expressed ChR2-YFP (Fig. 1C). Field potentials could be reliably evoked by a 473 nm blue laser in brain slices from these mice (Fig. 1D–E).

We tested two different methods of optogenetic stimulation. In the first method, an LSPS setup was used for precise and quick placement of the laser beam on a spot of the slice under the microscopic field. Most data presented in this paper were collected using this method. It also allowed us to scan a rectangular region of the slice to find a spot that evokes the maximum response (Fig. 1D). Changing the location of the laser flash caused corresponding changes in the waveform and amplitude of the evoked response. Moving the laser flash along the white matter did not result in systematic change in the amplitude of fEPSP. On-column optogenetic stimulation usually resulted in maximal fEPSP (−0.83 ± 0.01 mV in layer II/III), while moving the laser flash in layer V laterally away from a cortical column resulted in a decrease in the amplitude of fEPSPs (−0.69 ± 0.02 mV at 400 μm lateral). In contrast, moving the laser flash on-column from layer V towards to the recording pipette in layer II/III caused only small increases in the fEPSP amplitude. We also tested whether similar responses could be evoked by directly guiding the laser onto a target spot of a slice using a fiber optic. With the same laser intensity and duration, the responses evoked with the fiber optic were almost identical to these evoked by the LSPS setup (Fig. 1E), suggesting that it was feasible to use a fiber optic for oFPR.

The events of oFPR were generally comparable in amplitudes and waveform to those evoked with conventional electrodes, except that optogenetic fEPSPs often had two or more smaller peaks (Fig. 1D–E) and appeared later than those evoked by an electrode (Fig. 2A). In response to 0.1–1 ms laser stimulation of the white matter, the evoked responses in layer II/III typically started with a small amplitude stimulating artifact, followed by a peak of direct activation at ~3.3 ms (3.27 ± 0.05 ms), then a larger amplitude fEPSP (−0.81 ± 0.15 mV) with a mean peak latency of 7.7 ms (7.65 ± 0.06 ms), and finally a slow positive peak of fIPSP (Fig. 2B). In contrast, fEPSPs evoked by electrical stimulation had a mean amplitude of −0.7 mV (0.67 ± 0.05) after a mean latency of 4.3 ms (4.29 ± 0.16 ms). The mean onset latency of the optogenetically evoked fEPSPs was 4.95 ± 0.20 ms. We further recorded EPSPs in whole cell current recording mode from individual layer II/III pyramidal neurons by optogenetically stimulating layer V. The resulting EPSPs under different stimulating intensities had stable onset latency (4.82 ± 0.06 ms, Fig. 2C). The short and constant onset latencies of the EPSPs in the oFPR and whole cell recording suggest that the evoked fEPSPs were monosynaptic.

The components of the evoked events were confirmed pharmacologically. Addition of 20 μM AMPA receptor antagonist DNQX and 100 μM NMDA receptor antagonist APV almost completely blocked fEPSP and fIPSP events (Fig. 2D–E. Mean fEPSP: −1.16 ± 0.19 mV in normal ACSF and −0.16 ± 0.09 mV in APV+DNQX), but had no effect on the first peak. Addition of TTX in the perfusate resulted in complete blockage of the evoked response (Fig. 2D–E, mean fEPSP was −0.05 ± 0.03 mV in TTX). Addition of 10 μM bicuculline in the ACSF eliminated and reversed the third peak of the oFPR (Fig. 2F), suggesting that the third component was mediated by $GABA_A$ receptor activation. Addition of bicuculline also increased the amplitude and prolonged the decay time of the fEPSPs, likely reflecting an increase in network excitability due to disinhibition.

3.2 Stimulus and response relationship

To determine the relationship between the stimulus intensity and response, we recorded optogenetic field potentials by varying the intensity or duration of the laser pulses. At maximum laser intensity without attenuation, 1 ms laser pulse was measured at 0.04 mW in the LSPS system and 0.07 mW under the fiber optic. To determine the relationship between pulse duration and the evoked response, the laser pulses were applied without any

attenuation (0.04 mW, 1 ms). Gradual increases in pulse duration from 10 μs up to 5 ms resulted in corresponding increases in the peak amplitude of evoked fEPSPs, with the threshold of the pulse width being 50 μs and the maximum response being −2.1 mV (−1.46 ± 0.46 mV, n=5 slices. Fig. 3A). The maximum amplitudes of fEPSPs were achieved with 5 ms pulse duration at maximum intensity. To determine the relationship between laser power and the evoked response, 1 ms laser pulses with various laser intensities were applied. The threshold of laser power for evoking responses was 0.0012 mW. Increasing laser power (without change in pulse duration) resulted in increases in the amplitudes of fEPSPs, with a maximum response of −0.93 mV (−0.89 ± 0.03 mV, n=3 slices, Fig. 3B).

Long-duration optogenetic stimulation has been shown to cause desensitization of the ChR2 channels, which take up to 30 seconds for complete recovery (Mattis et al., 2012). To determine whether the short laser pulses used in our recording condition would also result in a depression of ChR2 channel activation, we measured the amplitudes of direction activation in layer II/III (Fig 2B, peak *b*) evoked by laser pulses at different frequencies (1 ms, 0.04 mW, 0.033 – 10 Hz). Laser pulses at 0.033 Hz did not result in a depression of the subsequent peaks, but higher stimulation frequencies (0.1 – 10 Hz) caused increasing depression of the peak amplitude of direct activation (Fig. 3C). To determine whether the desensitization would affect synaptic transmission, we further recorded fEPSPs in layer II/III evoked by different frequencies of laser pulses in layer V and calculated the paired pulse ratios by dividing the peak amplitude of the second fEPSPs by that of the first ones. The fEPSP2/fEPSP1 ratios were 1.0 ± 0.01, 0.98 ± 0.01, 0.95 ± 0.02, 0.90 ± 0, 0.86 ± 0.02, and 0.85 ± 0 at 0.033, 1, 2, 4, 10 and 20 Hz respectively (Fig. 3D). The small decreases in the fEPSP2/fEPSP1 ratios at higher stimulation frequencies suggested that desensitization of ChR2 channels does not significantly affect fEPSP at these stimulating frequencies.

3.3 Long term synaptic plasticity induced by optogenetic stimulation

Because of its “non-invasive” nature, optogenetic stimulation is expected to evoke consistent and stable field potentials in brain slice preparation, which could be particularly useful for studies that require repeated stimulation over an extended period of time such as in the recordings of long-term potentiation (LTP) and long-term depression (LTD). To determine the stability of oFPR over a long period of recording time, we recorded fEPSPs evoked by blue laser once every 30 seconds (0.033 Hz) for 60 minutes. The evoked fEPSPs were stable during the whole recording period (Fig. 4A). LTD of oFPRs in layer II/III was successfully induced by applying LFS protocol (1 Hz, 900 pulses) to layer V in 5 out of 8 slices (62.5%) (Fig. 4, n=5). Analysis of the depressed fEPSPs revealed a significant reduction of the mean peak amplitude at 60 minutes post-LFS to 55 ± 7 % of the baseline amplitude ($P<0.05$, paired *t*-test, Fig. 4). In contrast, optogenetic stimulation using 900 laser pulses at 2 Hz or 4 Hz did not induce LTD (Fig. 4C–D), which is consistent with the established frequency dependency of LTD induction (Kirkwood and Bear, 1994). As expected, laser pulses at classical theta burst or tetanus stimulation applied onto the white matter did not induce LTP in cortical layer II/III (5 slices, data not shown).

4. Discussion

We introduce a method of oFPR in brain slice preparation. Our results showed that extracellular field potentials could be reliably induced in layer II/III and layer V of neocortical slices by pulses of blue laser via the guidance of either a LSPS setup or simply a fiber optic. The typical events of oFPR consisted of a peak of short-latency non-synaptic ChR2 direct activation, followed by a mono-synaptic glutamatergic fEPSP and a GABAergic fIPSP. We further demonstrated that fEPSPs evoked by 0.033 Hz optogenetic stimulation remained stable during the 1–1.5 hour recording period and that it was feasible to use optogenetic LFS protocol to induce LTD in neocortical slices.

Although the responses from oFPR had comparable components and waveform as those evoked by electrical stimulation in the same slices (Fig 2A), there were small differences in the amplitude, latency, and waveform of the evoked fEPSPs between the two techniques. Because optogenetic stimulation only activates neurons and axons that express sufficient amount of channelrhodopsin-2, the population of activated axonal fibers and neurons must be different from those activated by an electrode. Therefore, we did not attempt to relate the oFPR response with the result of the conventional FPR. Previous patch clamp recording experiments demonstrated that optogenetic stimulation can reliably induce action potential firing by activating ChR2 channels in the somata or axons (Boyden et al., 2005; Petreanu et al., 2007; Wang et al., 2007). The relationships between the laser intensity or pulse duration and the evoked spikes are well characterized at single neuron level, and are generally consistent with our finding in oFPR (Fig. 3). Although short laser pulses also caused significant desensitization of ChR2 channels at the frequencies of 0.1 Hz and higher (e.g. 2^{nd} peak of direct activation depressed 58% at 10 Hz), the fEPSPs depressed only slightly at frequency up to 20 Hz (e.g. 2^{nd} fEPSP depressed 14% at 10 Hz, Fig. 3C–D). Because action potential firing can be reliably induced by laser pulses at up to 30 Hz in individual ChR2-expressing neurons under whole cell recording (Petreanu et al., 2007, Wang et al., 2007), and the depression of paired pulse ratios at higher stimulating frequencies are comparable to the results obtained with electrical stimulation in the neocortical slices(Castro-Alamancos and Connors, 1997, Pan et al., 2004), the change in paired pulse ratio in oFPR may similarly reflect a change in the probability of neurotransmitter release.

In comparison with the conventional FPR method that uses an electrode to evoke field potentials, the oFPR offers several unique advantages. First, because optogenetic stimulation activates only neurons and their axons that express ChR2-YFP, the origin of the evoked responses can be specifically defined by ChR2 expression in the presynaptic neurons. In the transgenic mice we used in this study, the cortical expression of ChR2-YFP was mostly in layer V, which allowed recording of field potentials that specifically originated from the cortical layer V. Second, optogenetic stimulation is non-invasive and highly reliable. It allows repeated stimulation over a long period of time, which is particularly useful for studying LTD and LTP, in which long-term monitoring of fEPSP is essential for the success of these experiments. Indeed, we found that LTD induction and monitoring using optogenetic stimulation were very stable throughout the period of the experiment. We were not able to induce LTP using regular 100 Hz LTP induction protocol, which was likely attributable to the fact that ChR2-YFP expressing pyramidal neurons can only fire action potentials at up to 35 Hz (Wang et al., 2007). However, recent studies suggested that neurons that express the second generation ultra-fast ChR2 constructs, such as ChETA, could be evoked to fire action potentials at much higher frequency (Gunaydin et al.). The use of such improved constructs may provide a solution for LTP induction in oFPR. Third, oFPR is more efficient and flexible. Using an LSPS system, a region of the slice can be systematically scanned to search for a spot that evokes maximum response or induces a specific response such as epileptiform activity. Using a fiber optic, the location of optogenetic stimulation can be changed simply by moving the fiber over the surface of the slice. Additionally, the small stimulus artifacts in oFPRs (Fig. 2) significantly improve the quality of recordings. These advantages make oFPR useful for studying the efficacy and plasticity of synaptic transmission.

Because the application of oFPR depends on the expression of ChR2 in specific neuronal population in certain brain regions, the level of ChR2 protein expression and its subcellular distribution will directly affect the amplitude and waveform of the evoked responses. These factors need to be taken into account and carefully controlled in a particular experiment so that a potential change in the level of ChR2 expression will not be interpreted as a change in the synaptic transmission. This may be particularly important under pathological conditions

such as brain injuries, in which changes in the expression and localization of certain proteins are frequently observed.

In summary, we introduce a method of oFPR. The technique allows reliable recording of evoked field potentials from brain regions that received input from genetically defined ChR2 expressing neurons. With the growing availability of various cell type–specific ChR2 transgenic mice (Zhao et al.) and new constructs for viral transfection, this technique will provide an efficient approach for studying synaptic transmission and its short-term and long-term plasticity in brain slice preparation.

Acknowledgments

We thank Xingjie Ping and Jianhua Gao for excellent technical support. This work was supported by the NIH grant NS057940 and the Indiana Spinal Cord and Brain Injury Fund to X.J.

Reference List

Arenkiel BR, Peca J, Davison IG, Feliciano C, Deisseroth K, Augustine GJ, Ehlers MD, Feng G. In vivo light-induced activation of neural circuitry in transgenic mice expressing channelrhodopsin-2. Neuron. 2007; 54:205–218. [PubMed: 17442243]

Barrionuevo G, Brown TH. Associative long-term potentiation in hippocampal slices. Proc Natl Acad Sci U S A. 1983; 80:7347–7351. [PubMed: 6316360]

Boyden ES, Zhang F, Bamberg E, Nagel G, Deisseroth K. Millisecond-timescale, genetically targeted optical control of neural activity. Nat Neurosci. 2005; 8:1263–1268. [PubMed: 16116447]

Castro-Alamancos MA, Connors BW. Distinct forms of short-term plasticity at excitatory synapses of hippocampus and neocortex. Proc Natl Acad Sci U S A. 1997; 94:4161–4166. [PubMed: 9108122]

Gunaydin LA, Yizhar O, Berndt A, Sohal VS, Deisseroth K, Hegemann P. Ultrafast optogenetic control. Nat Neurosci. 13:387–392. [PubMed: 20081849]

Histed MH, Bonin V, Reid RC. Direct activation of sparse, distributed populations of cortical neurons by electrical microstimulation. Neuron. 2009; 63:508–522. [PubMed: 19709632]

Jin X, Huguenard JR, Prince DA. Reorganization of inhibitory synaptic circuits in rodent chronically injured epileptogenic neocortex. Cereb Cortex. 2011; 21:1094–1104. [PubMed: 20855494]

Jin X, Prince DA, Huguenard JR. Enhanced excitatory synaptic connectivity in layer v pyramidal neurons of chronically injured epileptogenic neocortex in rats. J Neurosci. 2006; 26:4891–4900. [PubMed: 16672663]

Kimura F, Nishigori A, Shirokawa T, Tsumoto T. Long-term potentiation and N-methyl-D-aspartate receptors in the visual cortex of young rats. J Physiol. 1989; 414:125–144. [PubMed: 2575160]

Kirkwood A, Bear MF. Homosynaptic long-term depression in the visual cortex. J Neurosci. 1994; 14:3404–3412. [PubMed: 8182481]

Mattis J, Tye KM, Ferenczi EA, Ramakrishnan C, O'Shea DJ, Prakash R, Gunaydin LA, Hyun M, Fenno LE, Gradinaru V, Yizhar O, Deisseroth K. Principles for applying optogenetic tools derived from direct comparative analysis of microbial opsins. Nat Methods. 2012; 9:159–172. [PubMed: 22179551]

Pan B, Yang DW, Han TZ, Xie W. Changes in the paired-pulse ratio after long-term potentiation induced by 2- and 100-Hz tetanus in rat visual cortical slices. Brain Res. 2004; 1021:146–150. [PubMed: 15328043]

Petreanu L, Huber D, Sobczyk A, Svoboda K. Channelrhodopsin-2-assisted circuit mapping of long-range callosal projections. Nat Neurosci. 2007; 10:663–668. [PubMed: 17435752]

Prince DA, Tseng GF. Epileptogenesis in chronically injured cortex: in vitro studies. J Neurophysiol. 1993; 69:1276–1291. [PubMed: 8492163]

Renshaw B, Forbes A, Morison BR. ACTIVITY OF ISOCORTEX AND HIPPOCAMPUS: ELECTRICAL STUDIES WITH MICRO-ELECTRODES. Journal of Neurophysiology. 1940; 3:74–105.

Wang H, Peca J, Matsuzaki M, Matsuzaki K, Noguchi J, Qiu L, Wang D, Zhang F, Boyden E, Deisseroth K, Kasai H, Hall WC, Feng G, Augustine GJ. High-speed mapping of synaptic connectivity using photostimulation in Channelrhodopsin-2 transgenic mice. Proc Natl Acad Sci U S A. 2007; 104:8143–8148. [PubMed: 17483470]

Wang J, Wagner F, Borton DA, Zhang J, Ozden I, Burwell RD, Nurmikko AV, van Wagenen R, Diester I, Deisseroth K. Integrated device for combined optical neuromodulation and electrical recording for chronic in vivo applications. J Neural Eng. 2007; 9:016001. [PubMed: 22156042]

Zhang J, Laiwalla F, Kim JA, Urabe H, Van Wagenen R, Song YK, Connors BW, Zhang F, Deisseroth K, Nurmikko AV. Integrated device for optical stimulation and spatiotemporal electrical recording of neural activity in light-sensitized brain tissue. J Neural Eng. 2009; 6:055007. [PubMed: 19721185]

Zhao S, Ting JT, Atallah HE, Qiu L, Tan J, Gloss B, Augustine GJ, Deisseroth K, Luo M, Graybiel AM, Feng G. Cell type-specific channelrhodopsin-2 transgenic mice for optogenetic dissection of neural circuitry function. Nat Methods. 2011; 8:745–752. [PubMed: 21985008]

Highlights

Field potential recordings were reliably evoked with optogenetic stimulation in brain slices of Channelrhodopsin2 expressing transgenic mice. Tow techniques of optogenetic stimulation are introduced and tested. Optogenetic fiend potential recording can be used for the induction of long-term depression.

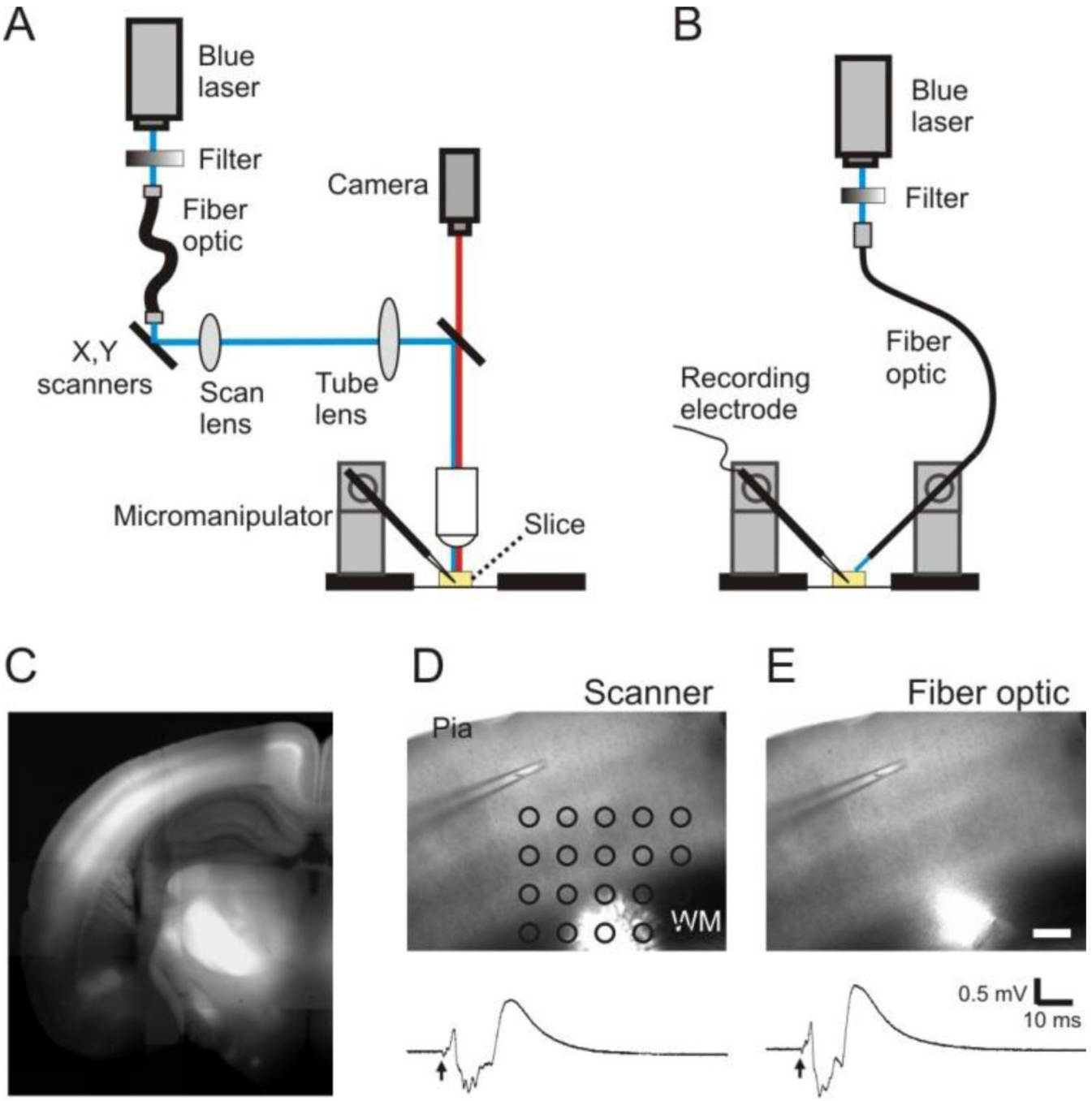

Figure 1.

A method of oFPR. **A** and **B**: Schematic representation showing that a laser scanning photostimulation system (A) or a fiber optic attached to a micromanipulator (B) was used for delivering pulses of blue laser (473 nm) onto brain slices. **C**. A fluorescence image of a coronal cortical slice prepared from a ChR2-YFP expressing transgenic mouse. ChR2-YFP expression is clearly visible in the cortex, particularly in layer V and layer II/III. **D** and **E**: Optogenetic stimulation delivered with the methods illustrated in either A (1-ms laser pulse at 0.04 mW) or B (1-ms laser pulse at 0.07 mW) evoked similar responses. Arrows indicate the time of laser flashes. Scale bar in E: 200 μm.

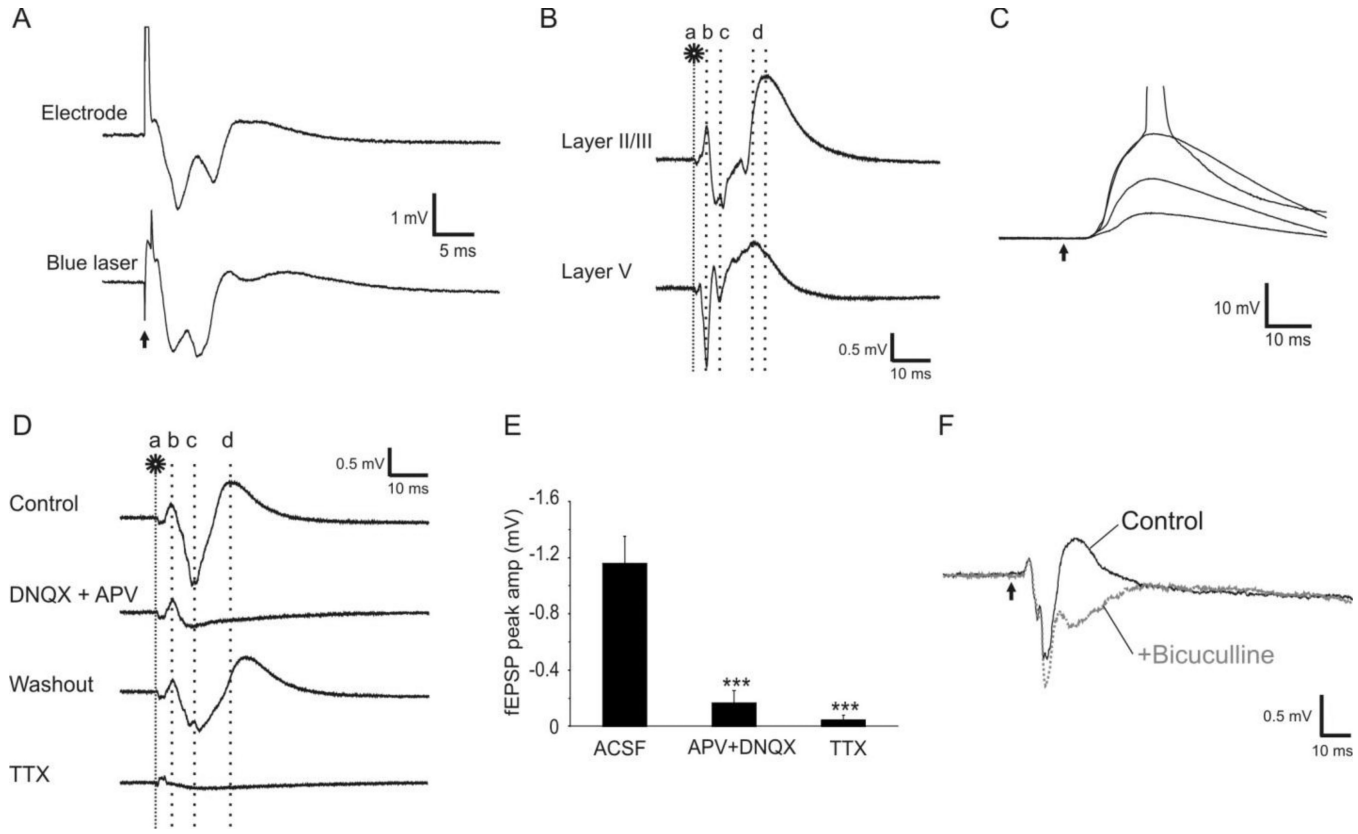

Figure 2.

Field potentials evoked by optogenetic stimulation. **A**. Extracellular field potentials evoked in cortical layer II/III by electrical (0.2-ms pulse of square current at 0.5 mA, top trace) or optogenetic (2-ms pulse of blue laser at 0.04 mW, bottom trace) stimulation of the white matter. **B**. The components of optogenetically evoked responses: Following a laser flash on the white matter (*a*, 1 ms at 0.04 mW), the first negative (layer V) or positive (Layer II/III) peak appeared at 3.3 ms (*b*), which resulted from direction activation of ChR2 expressing axons. The second peak(s) of fEPSP occurred at ~7.1ms (*c*), which was followed by a slower large positive peak of fIPSP (*d*). **C**. Whole cell current clamp recording was made from a layer II/III pyramidal neuron when laser pulses at increasing intensities (1 ms, 0.01–0.04 mW) were applied to layer V. The constant onset latency of the evoked EPSPs indicates the monosynaptic nature of the responses. The action potential trace is truncated for better demonstration of the EPSPs. D–F. Pharmacology of optogenetically evoked responses. **D**. Addition of AMPA and NMDA receptor antagonists DNQX (20 μM) and APV (100 μM) blocked fEPSP (*b*) and fIPSP (*c*) but not the direct activation (*a*). This blockade was reversible by washing with normal ACSF. Application of 1 μM TTX abolished almost all components of the evoked response (bottom trace). **E**. The effects of those drugs on the fEPSP peak amplitudes (−1.16 ± 0.19 mV in control; −0.16 ± 0.09 mV in APV + DNQX, and −0.05 ± 0.03 mV in TTX, ***: $P < 0.001$). **F.** Addition of 10 μM $GABA_A$ receptor antagonist bicuculline in the ACSF blocked the third outward peak (gray trace), confirming that this component was an IPSP. The arrow indicates the time of laser flash.

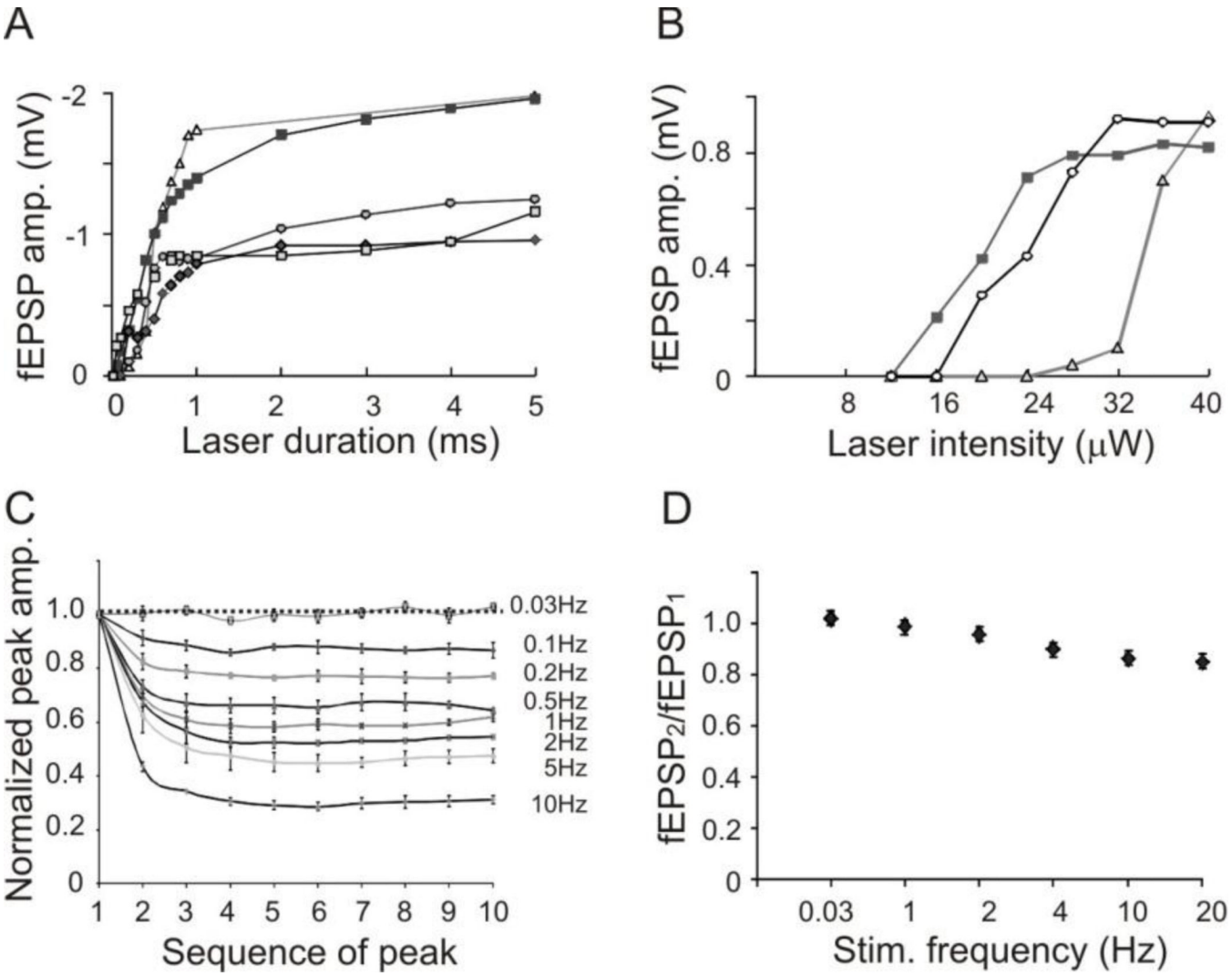

Figure 3.

Relationships between parameters of optogenetic stimulation and the evoked responses. **A**. Relationship between laser duration at maximum intensity (0.04 mW) and peak amplitude of evoked fEPSPs. **B**. Relationship between laser intensity of 1 ms pulses and peak amplitude of evoked fEPSPs. In both A and B, each line represents recordings from a slice. **C**. Significant desensitization of ChR2 activation at higher stimulating frequencies: The peak amplitudes of direct activation (peaks *b* in Fig. 2B) recorded in layer II/III rapidly depressed with increasing stimulating frequency. **D.** Relationship between fEPSP2/fEPSP1 ratio and stimulating frequency. Optogenetically evoked fEPSPs only slightly depressed at higher stimulating frequencies.

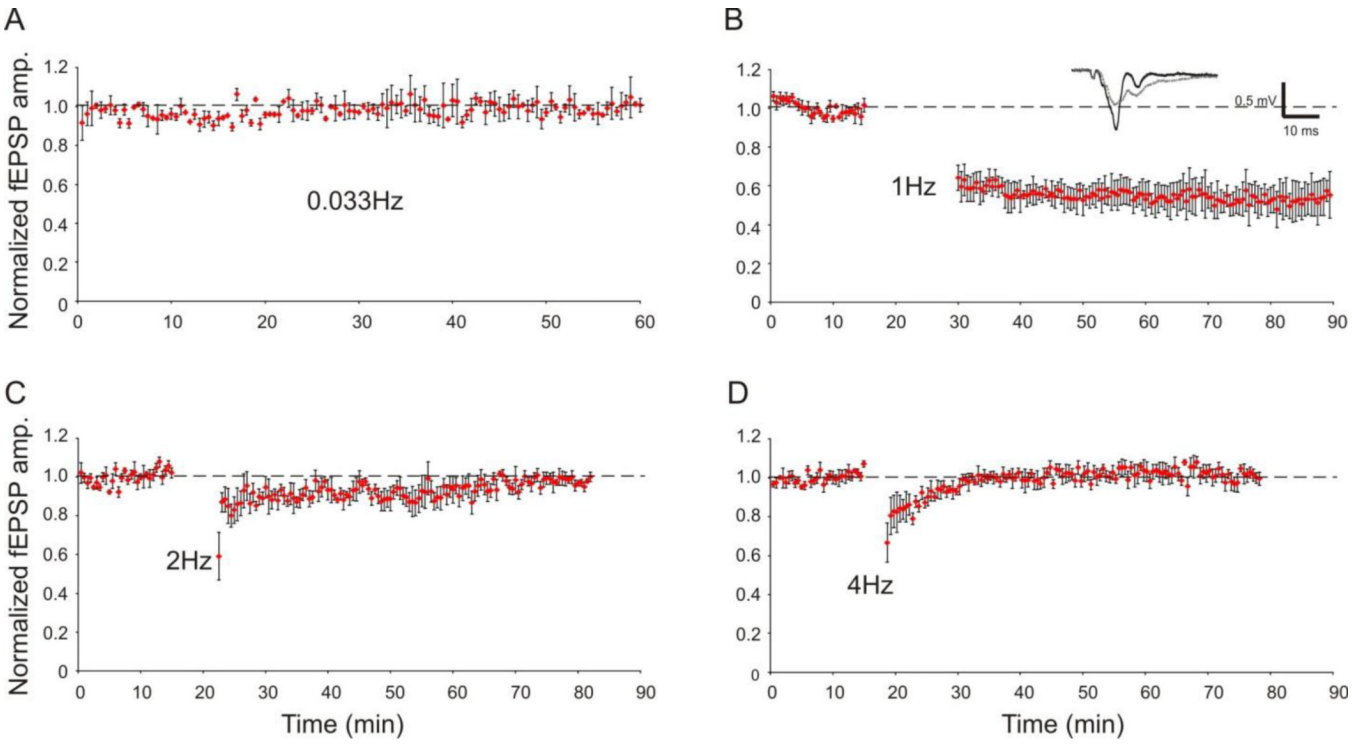

Figure 4.

Stability of oFPR and optogenetic induction of LTD. Field potentials were elicited in layer II/III by applying laser flashes in layer V (1 ms at 0.04 mW). **A**. Normalized fEPSP amplitudes evoked by pulses of blue laser at 0.033 Hz were stable throughout the 60-min recording period (n=3). **B–D**. LTD induction by LFS: The graphs show normalized fEPSP peak amplitudes recorded before and after conditioning stimulation (900 pulses) at 1 Hz (B, n=5), 2 Hz (C, n=4), or 4 Hz (D, n=4). Only optogenetic stimulation at 1 Hz resulted in long-term depression of fEPSP amplitude (B), suggesting that the optogenetic LTD induction was frequency-dependent. Insert in B: representative average field potential traces before (black trace) and after (gray trace) LFS in a slice.